View metadata, citation and similar papers at core.ac.uk

brought to you by CORE

provided by NOPR

Indian Journal of Engineering & Materials Sciences
Vol. 27, April 2020, pp. 373-381

Effect of laser remelting on the microstructure and mechanical properties of meta inert gas welded low carbon mild steel

Sathyavageeswaran Sathish*

Department of Mechanical Engineering, Aalim Muhammed Salegh College of Engineering, Avadi IAF, Chennai-600055, India

Received: 12 November 2018 ; Accepted: 11 march 2020

In this study, laser remelting has been performed on the Metal Inert Gas welded (MIG) low carbon mild steel at varying laser power inputs (400 W & 600 W). To investigate the influence of laser remelting on the joint properties, optical microscope observation, scanning electron microscope observation, microhardness measurement and mechanical tests have been conducted. The experimental results revealed that the surface appearance of the laser remelted MIG welded joints have been found to be smooth and the microstructure of its fusion zone possesses fine equiaxed dendrites as compared with that of the MIG welded joints. In addition, the fracture surface of the laser melting carried at low power (400 W) on the MIG welded joint has exhibited a ductile fracture whereas, the MIG welded joint has undergone brittle fracture. The laser remelting carried out at 400 W on the MIG welded joint has resulted in 12% increase in both the ultimate tensile strength and percentage of elongation as compared to that of the MIG welded joint and this has been ascribed to the presence of equiaxed grains in the microstructure.

Keywords: Laser remelting, Microstructure; Hardness, Tensile test, Fractography

1 Introduction

Metal Inert Gas welding (MIG) has been traditionally employed for joining low carbon mild steel which is being often used in the construction of bridges, ships and automobile applications[1-5]. Previous studies have revealed that the toughness of the weldment is greatly reduced by the formation of more than 77% ferrite phase in the low carbon mild steel[6]. Besides, the mechanical properties of the arc welded joints were affected due to the presence of coarse grains and wider heat affected zone[7,8]. Hence, refinement of grains in the weldment is of prime importance. Several grain refinement techniques such as weld pool stirring, electromagnetic stirring, ultrasonic vibration, Arc pulsation and Arc oscillation are available to counteract the above effect[9-11]. Jia Liu *et al.* have performed ultrasonic vibration in Laser-MIG hybrid welding and observed a significant refinement in the microstructure which in turn has led to the higher tensile strength of the joint[12]. The treatment of the pulse current on the Gas Metal Arc Welded Joints has restrained the dendritic growth resulting in fine grains[13]. The microstructure of AZ series Mg alloys welded by arc welding with or without ultrasonic vibration is studied and the mechanisms of grain refinement in the welding process are discussed in detail[14]. The influence of various process parameters like the Voltage applied, Current, Welding speed have been studied extensively and the various response output obtained based on its microstructure, fatigue resistance have been critically assessed by Rishav Sen *et al.* [15]. The research work carried out by Gural *et al.*. have suggested that the increase in welding parameters, such as Heat Input and Welding speed can also results in the formation of equiaxed grains[16]. Senthil kumar *et al.* have demonstrated that the presence of equiaxed grains in the microstructure of welded AA 6061 Aluminium has led to significant improvement in the tensile strength[17]. Most recent work carried out by Devandranath Ramkumar *et al.* have demonstrated that the low energy shock peening carried out in the Haste alloy C-276 welds have resulted in the remarkable improvement of tensile strength of the welded joints by shifting the location of tensile failures away from the fusion zone[18]. Despite, several routes are available to refine the microstructures of the weldments; laser surface remelting can be considered as the best technique as it has received much attention in modifying the surface of plasma sprayed ceramic coatings. For instance, it is obvious from various studies that the laser remelting plays a

*Corresponding author (E-mail: mechhh_er@rediffmail.com)

crucial role in modifying the lamellar structure of plasma sprayed coatings into equiaxed grains which is well preferred for enhancing the mechanical properties and in addition to this, the pores generated in the coating can be reduced to the maximum extent[19-22]. Despite the fact that laser remelting technique has been effectively utilized for refining the microstructure of the plasma sprayed ceramic coatings, hitherto laser remelting has not been employed over the surface of the weldments. Hence, this work is first of its kind wherein laser remelting was carried out on the top surface of the MIG welded joints and its microstructural features and mechanical properties are discussed in detail.

2 Experimental procedure

2.1 Sample Preparation

AISI 1018 Low carbon mild steel having a chemical composition as shown in Table 1 has been machined to a dimension of 75 mm x 60 mm x 5 mm using wire cut machine. Later the specimens were polished using 220 micron grit size emery sheet and cleaned by acetone to avoid contaminants.

2.2 MIG Welding and Laser Remelting

A semi automatic Metal Inert Gas (MIG) machine was utilized to perform Bead on plate welding on low carbon mild steel. Argon was used as a shielding gas. A standard AWS-ER 70S-6 filler wire having a diameter of 1.2 mm was chosen. The parameters employed for MIG welding is provided in Table 2. Laser remelting was performed on the top surface of the MIG welded low carbon mild steel approximately to a depth of 2 mm with a Robot controlled continuous wave CO_2 laser (HUST-JKT5170) operating at a wavelength of 10.6 µ m with a maximum output power of 5 kW. Nitrogen was used as a shielding gas to prevent the formation of oxides on the welded region. Laser remelting was performed on the MIG welded joints by varying the laser power and scanning speed and the optimized parameters are shown in Table 3. The MIG welding setup is shown in Fig.1.

Table 1 — Composition of base metal.

Elements	Composition (wt.%)
Carbon	0.11
Manganese	0.72
Phosphorous	0.026
Sulphur	0.039
Iron	99.105

Table 2 — Parameters for MIG welding.

Welding Conditions	
Voltage	30 V
Shielding gas	Argon
Electrode	AWS-ER 70S-6 filler wire
Electrode diameter	1.2 mm
Gun to work piece	8 mm
Weld speed	11 mm/s
Flow rate	12 l/m

2.3 Microstructural Analysis

The welded samples are sectioned to a convenient size, it is mounted in a epoxy material to facilitate handling during the grinding and polishing steps. Mounting media must be compatible with the sample in terms of hardness and abrasion resistance. Polishing was performed using different grit size emery sheets of 220 µm, 400 µm, 600 µm, 800 µm and 1000 µm and subsequently polished using 0.5 µm diamond paste to obtain good surface finish and finally etched by a solution of aqua regia ($HCl:HNO_3$ = 3:1). Later, the weld joint structures and its cross sectional shapes were examined using Carl Zeiss Optical microscope.

2.4 Mechanical Properties

The Schematic diagrams of Vickers Hardness tester and Universal Testing Machine are shown in Fig.2(a&b). Vickers hardness testing was performed across the welded joints by applying a load of 100g

Table 3 — Parameters for laser remelting.

S.No	Laser power(W)	Scanning speed (mm/s)	Spot size(mm)
1	400	15	3
2	600	15	3

Fig. 1 — Set-up of MIG welding process.

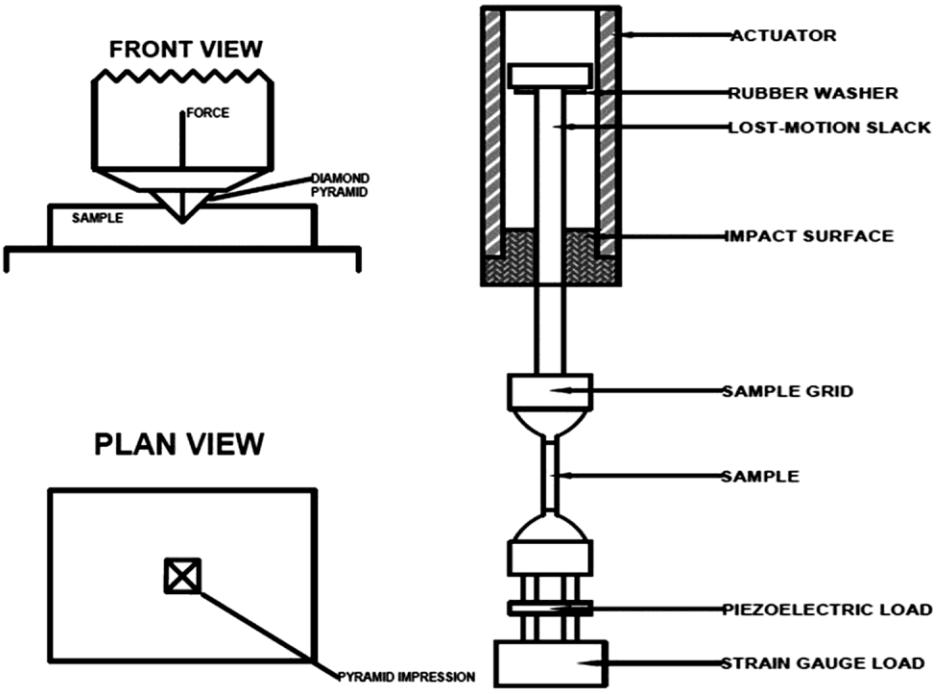

Fig. 2 — Schematic diagrams of (a) Vickers hardness tester and (b) Universal testing machine.

for 15 s. Tensile testing was performed on the specimens using INSTRON 5569 universal testing machine at a loading rate of 1 mm/min. The stress vs. strain curves were monitored by a data acquisition system through a standard load cell and strain gauge and the tensile strength reported is the average of the three values. Fractography analyses of the samples were carried out using Scanning electron microscope (SEM, JEOL JSM-6360).

3 Results and Discussion

3.1 Appearance of Welded Joints

The top and bottom views of the MIG and laser re-melted MIG welded joints are depicted in Fig. 3 (a-f). It is evident from Fig. 3 (a&b) that the MIG welded joint was found to be smooth and no pores and cracks were noticed. Furthermore, a silvery white color was observed across the weld bead signifying that the Argon gas has shielded the molten pool from oxidation. However, a thin layer was noticed along the edges of the welded joint depicting that oxidation has taken place as the Argon gas has moved away. Unlike MIG welding, few minute pores were observed on the surface of laser remelted MIG welded joints (Fig.3 (c&e)).This is mainly due to the fact that the intensity of laser power input has increased the weld pool surface temperature much above the boiling points of the materials which in turn resulting in higher equilibrium pressure on the weld pool surface than the atmospheric pressure thereby pushing the liquid metal from the weld pool surface leading to few pores. These results are well in concurrent with that of the results reported by Cu *et al.*.[23]

3.2 Cross-sectional Shape of Welded Joints

The cross sectional morphologies of the welded joints are shown in Fig.4 (a-c). It is obvious that the shape of the weld bead was narrow at the top and wider at the bottom for all the three specimens and this is in contradictory with that of the shapes reported by several authors[4,24,25]. However, the laser remelted MIG welded joints shows a slightly protruded surface. This is due to fact that the existence of high equilibrium pressure across the melt pool has expelled the molten metal towards the top leading to the formation of spatter. Moreover, a thick layer of heat affected zone (HAZ) was observed surrounding the weld zone of laser remelted MIG welding carried out at 600 W (Fig.4 (b)). Conversely, the laser remelting carried out at low laser power (400 W) has generated higher cooling rate which in turn has restricted the growth of the grains surrounding the weld zone thereby resulting in thin or very little HAZ (Fig.4(c)).

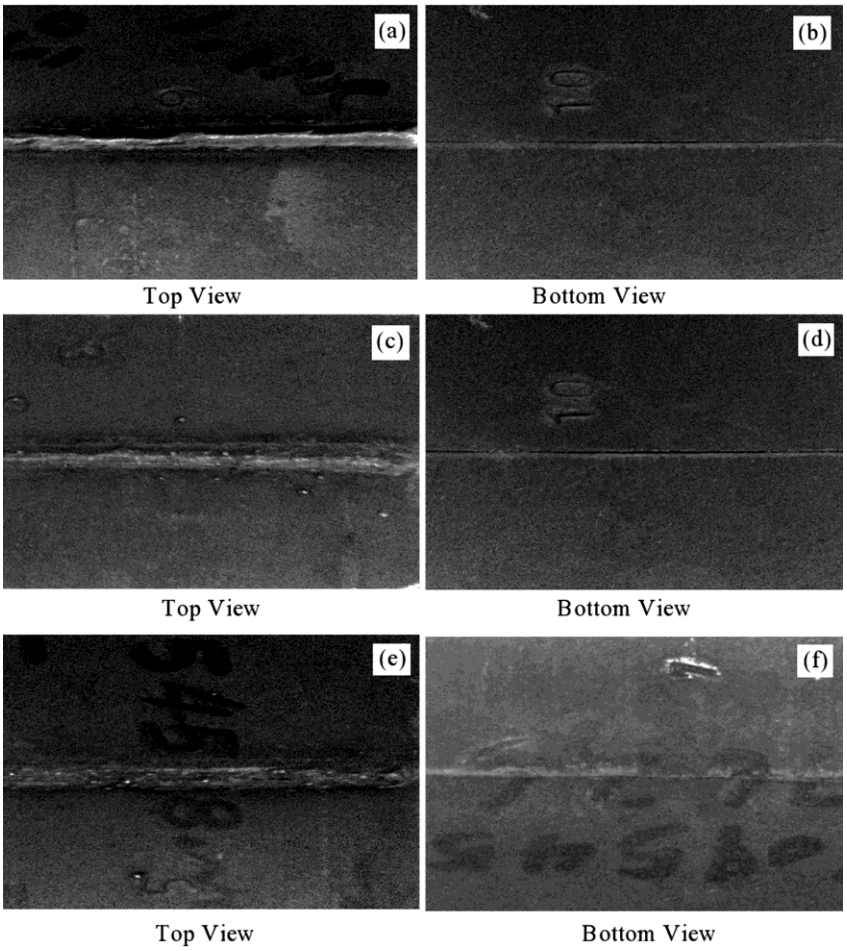

Fig. 3 — Typical weld joint appearances: (a&b) MIG welding, (c&d) laser remelted MIG welding (Power: 400 W), (e&f) laser remelted MIG welding (power: 600 W).

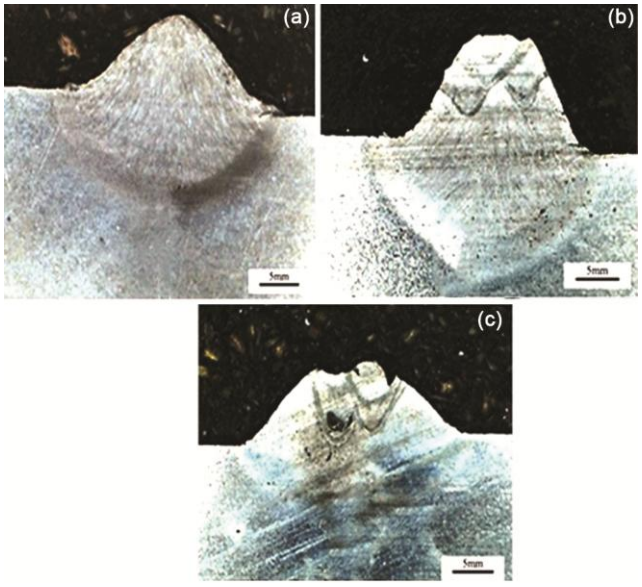

Fig. 4 — Cross sectional morphologies of (a) MIG welding and (b) Laser remelted MIG (Power :600 W) and laser remelted MIG (power: 400 W).

3.3 Microstructure of MIG and Laser Remelted MIG Welded Joints

The optical micrographs of the MIG welding clearly reveals the presence of different zones such as Parent metal, Heat affected zone and Fusion zone (Fig.5 (a-d)). Few pearlite (dark region) dispersed in the ferrite matrix (light region) was observed in the Parent metal of MIG welded joint depicting low carbon steel (Fig.5 (b)).The heat affected zone consisted of more amount of pearlite with few ferrites. Moreover, the rapid solidification involved in the Parent metal has resulted in the formation of finer grains (Fig.5(c)). The fusion zone shows the presence of large number of columnar dendrites comprising of ferrite and pearlite growing perpendicular to the molten metal and this is ascribed to the rapid cooling from liquid to solid state involved in the process (Fig.5(d)).

The heat affected zone (HAZ) and parent metal of the laser remelted MIG welding carried out at varying

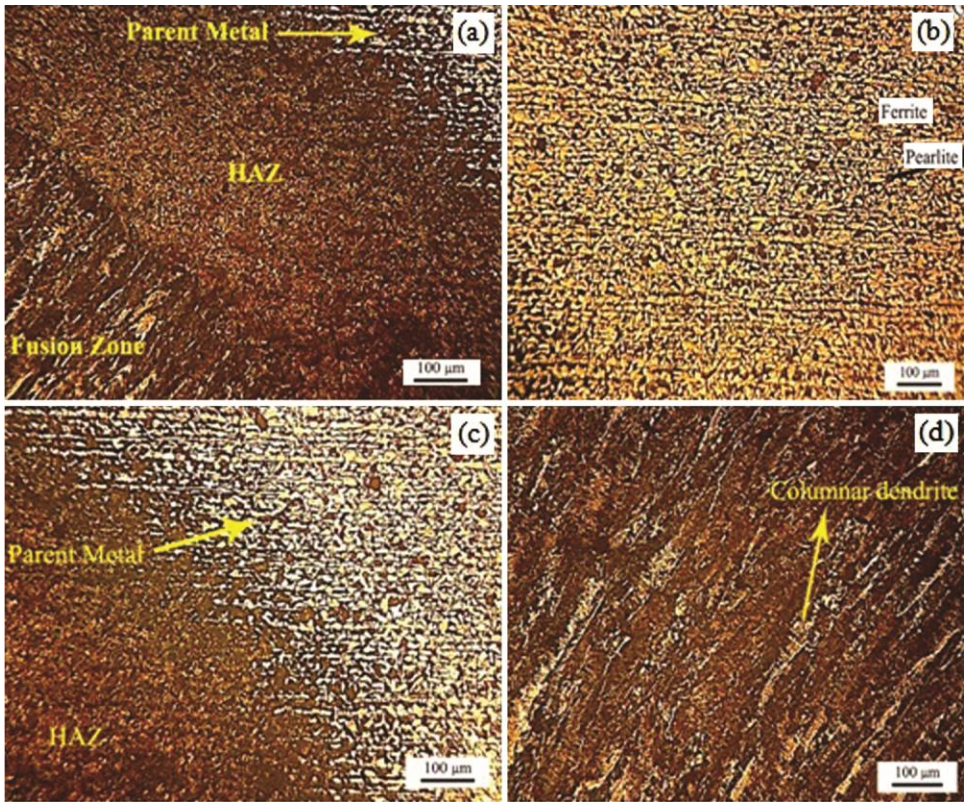

Fig. 5 — Microstructure of MIG welded joint (a) overall view, (b) Parent metal, (c) Combination of HAZ & parent metal and (d) Fusion zone.

power inputs (400 W & 600 W) show similar microstructures as that of the MIG welded joint (Figs.6(a)&7(a)). However, the pearlite grains observed in the HAZ have undergone recrystallization and resulted in fine grains. Also, the size of the dendrites observed on both the laser remelted MIG welded joints were found to be smaller when compared with that of the fusion zone of the MIG welded joints (Figs6(b)&7(b)). Moreover, the dendrites observed on both the laser remelted surface were equiaxed when compared with that of the MIG welded joint (Figs.6(c) &7(c)). The reason for this is that the irradiation of laser beam over the welded joints has increased the solidification rate which in turn has resulted in very fine equiaxed dendrites.

3.4 Hardness

The micro hardness measured across various regions such as fusion zone, heat affected zone and the parent metal are shown in Fig. 8. It is obvious that the fusion zone of the MIG welded possesses maximum hardness of 305 HV (Standard Error:11.15) and this could be attributed to the presence of columnar dendrites. On the other hand, the presence of fine equiaxed dendrites in the fusion zone of the laser remelted MIG welded joints at 600 W have resulted in lower hardness of 284 HV(Standard Error : 8.39). The reason for higher hardness of the MIG welded joint is ascribed to the high dislocation density in the columnar dendrites when compared with that of the equiaxed dendrites as reported by Sakthivel *et al.*[26]. Further, the drop in hardness across the HAZ of both the laser remelted MIG welding (400 W& 600 W) is attributed to the retention of more amount of heat on its surface. Thus the hardness values are well in accordance with that of the microstructural features reported earlier.

3.5 Tensile Testing and Fractography

The ultimate tensile strength and Percentage of Elongation of the welded joints are presented in Table 4. It is clear that there has been a marginal increase in ultimate tensile strength and Percentage of Elongation of laser remelted welded joints when compared with that of the MIG welded joints. Figure 9 depicts the macroscopic fracture surface of

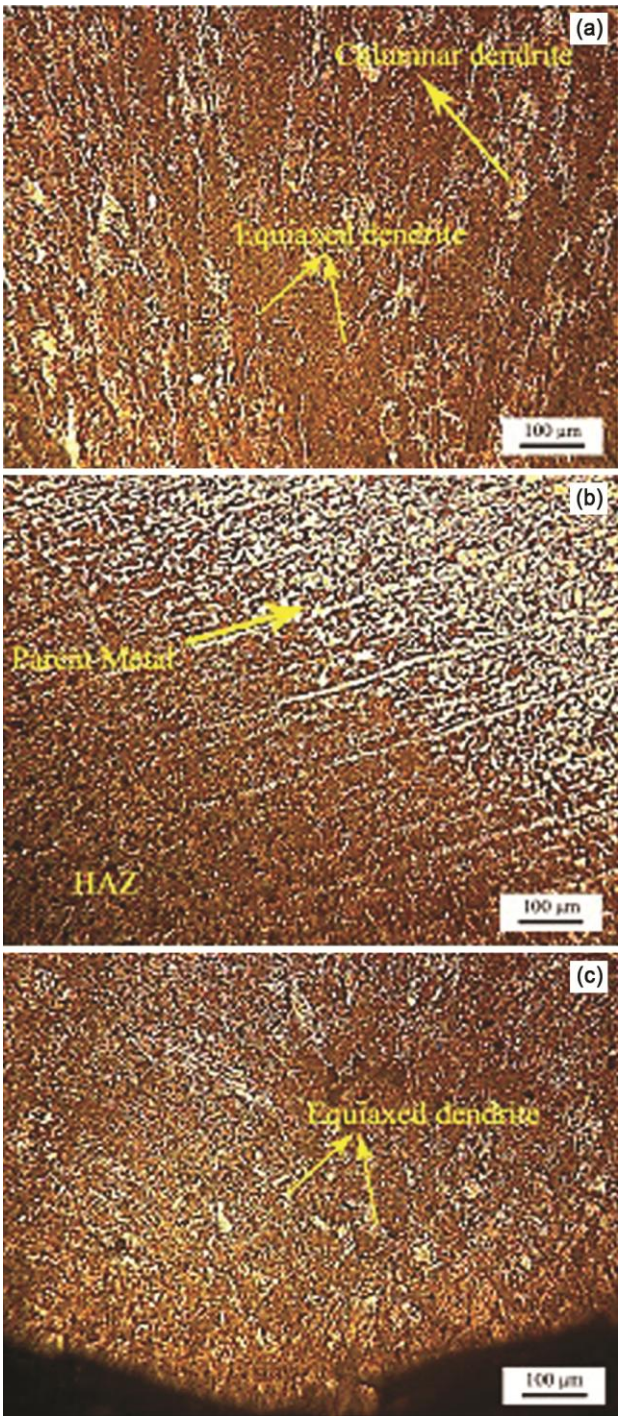

Fig. 6 — Microstructure of laser remelted MIG welded joint at 600 W (a) Combination of HAZ and parent metal, (b) Fusion zone and (c) Laser remelted zone.

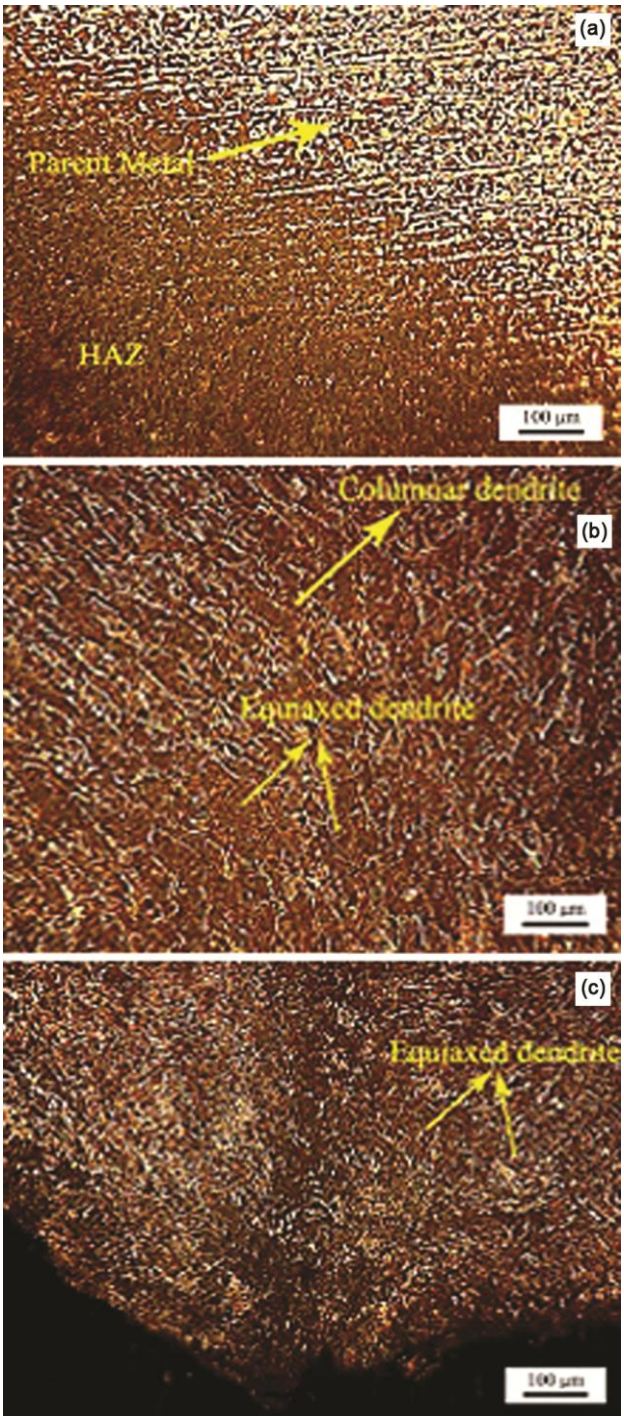

Fig. 7 — Microstructure of laser remelted MIG welded joint at 400 W (a) Combination of HAZ and parent metal, (b) Fusion zone and (c) Laser remelted zone.

the welded joints. From the macroscopic observation, it is evident that both the laser remelted MIG welded joints fractured and the forced direction form an angle of 45^{o} in the shape of shearing type ductile fracture. This result is well in corroboration with that of the fractured surface of the hybrid laser- MIG welded joints reported by Shaohua Yan *et al.*.[27] where as the MIG welded joint has undergone brittle fracture. However, in order to examine the modes of fracture encountered in the welded joints, fractured surface

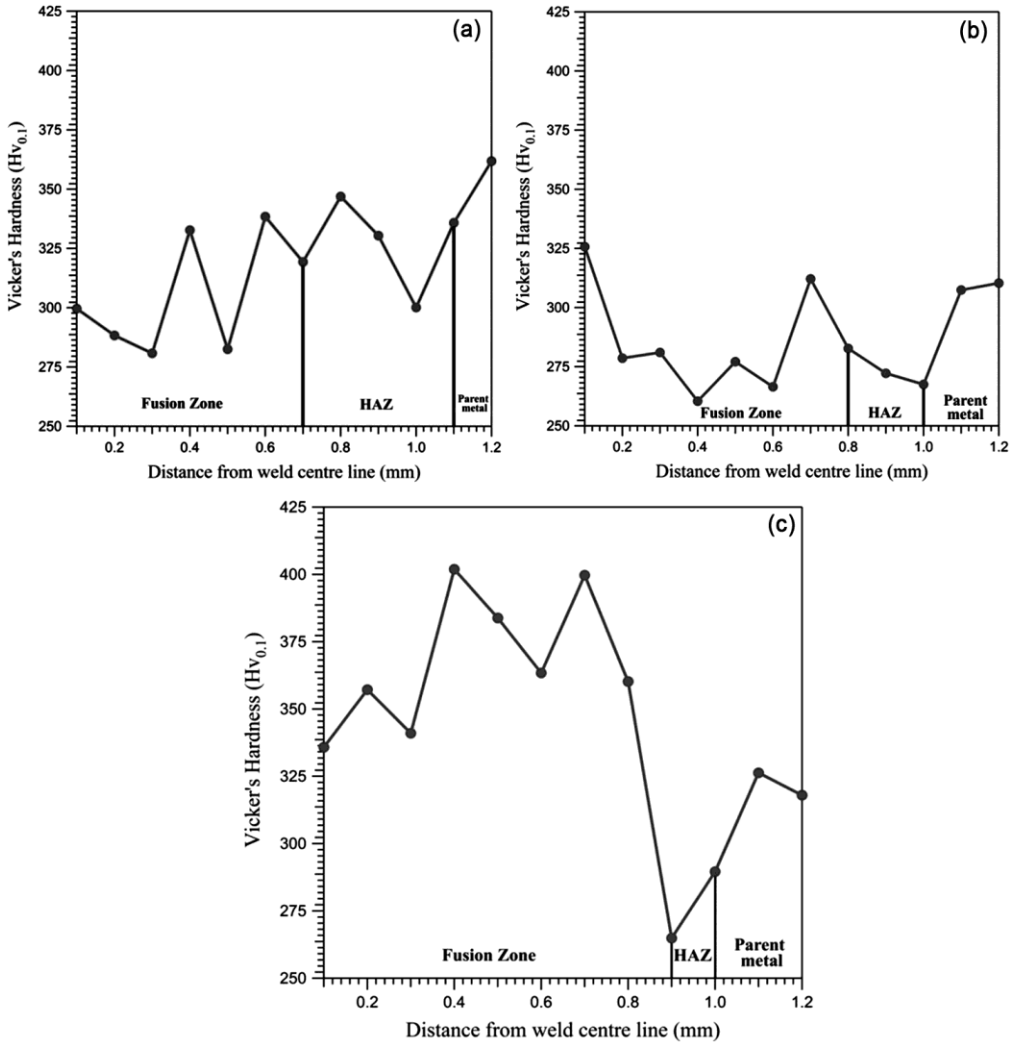

Fig. 8 — Microhardness of (a) MIG welded joint, (b) Laser remelted MIG (600W) and (c) Laser remelted MIG (400W).

Table 4 — Tensile properties of welded joints.

Joint type	Hardness Ultimate tensile $(HV)_{0.1}$ strength (MPa) (± % error)	(±% error)	Percentage of Elongation
MIG welded joint	305 (11.15)	445 (2.33)	16.5
Laser remelted MIG welded joint: 600 W	284 (8.39)	487 (3.61)	18
Laser remelted MIG welded joint :400 W	302 (14.48)	502 (2.52)	18.5

were analyzed using SEM. It is evident from Fig.10 (a) that the fracture appearance of the laser remelted MIG welding carried out at 400 W shows greater number of dimples with micro void coalescence depicting typical ductile fracture. This result is well in accordance with that of the fracture surface obtained during the friction stir welding of Mild steel as reported by Lakshminarayanan *et al.*[28]. On the other hand,

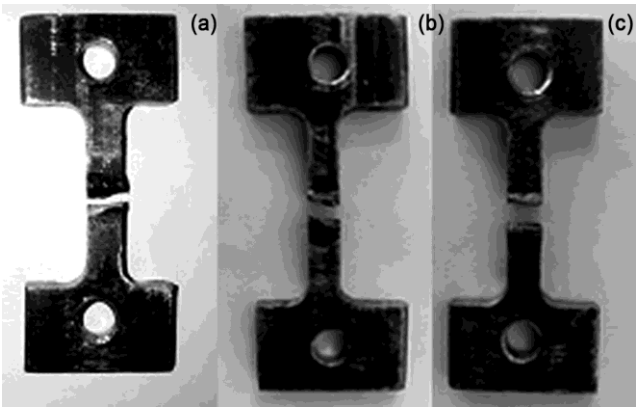

Fig. 9 — Macroscropic view of tensile tested sample (a) Laser remelted MIG welded joint (400 W), (b) Laser remelted MIG welded joint (600 W) and (c) MIG welded joint.

the dimples observed on the fracture surface of the laser remelted joint carried out at 600 W (Fig.10 (b))

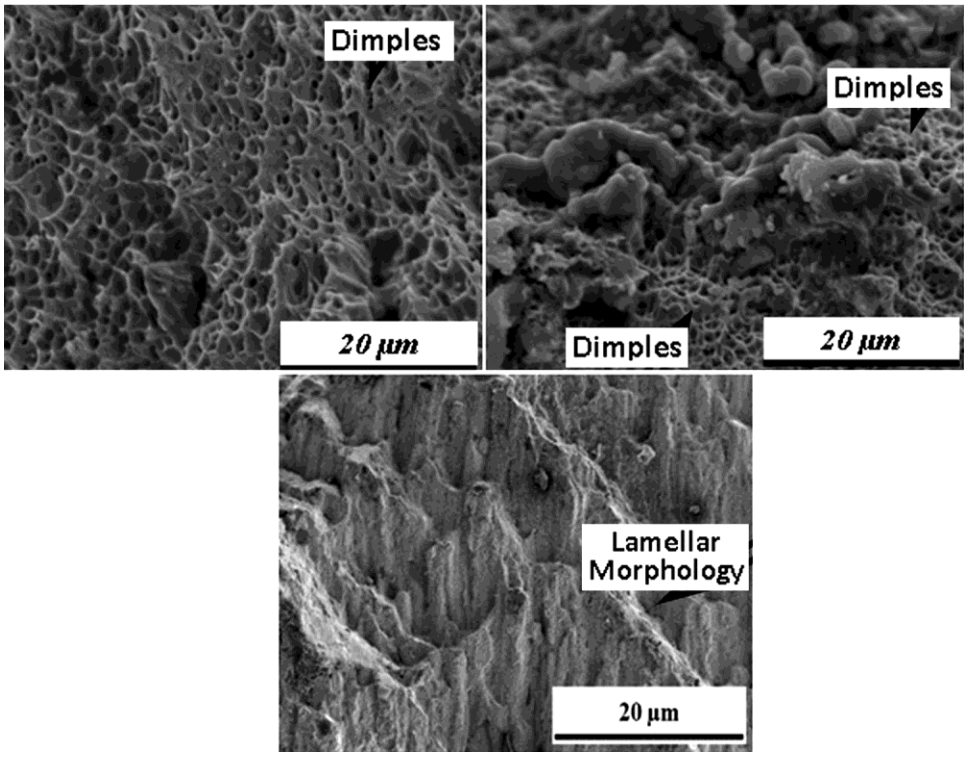

Fig.10 — Fracture surface morphologies of (a) laser remelted MIG welding (400 W), (b) laser remelted MIG welding (600 W) and (c) MIG welding.

was found to be reasonably small and fraction of it belongs to brittle fracture signifying mixed mode of fracture characteristics. The existence of fine pearlite in the equiaxed dendrites of the laser remelted joints have resulted in ductile fracture. The fracture appearance of the MIG welded joint (Fig.10(c)) exhibited lamellar morphology without severe deformation implying brittle fracture. This is mainly due to the accumulation of stresses in the columnar dendrites. Similiar result was observed by Caiwang Tan et.al during the laser-tungsten inert gas hybrid welding of dissimilar metals AZ31B Mg alloys to Zn coated steel[29].

4 Conclusions

The microstructure and mechanical properties in the MIG and laser remelted joints were examined and the following conclusions were drawn.

(i) The weld appearances of all the joints were found to be smooth, continuous and crack free.

(ii) Laser remelted joint processed at 400 W consisted of a very thin layer of HAZ as compared with that of other two joints and the fine equiaxed dendrites were predominant in the fusion zone of laser remelted joints.

(iii) The MIG welded joint showed 8% increase in the hardness as compared with that of the laser remelted MIG welded joints at 600 W and this is ascribed to the presence of columnar dendrites**.**

(iv) The effect of laser remelting performed at 400 W on the MIG welded joint has resulted in 12% increase in ultimate tensile strength as compared with that of the MIG welded joint and this is ascribed to the presence of equiaxed grains in the microstructure.

(v) Laser remelting performed at 400 W on the MIG welded joint has led to 12% increase in percentage of elongation than that of the MIG welded joint and 2.7 % increase as compared to that of the laser remelted MIG at 600 W.

(vi) The laser remelted MIG welded joints have shown better combination of strength and ductility as compared with that of MIG welded joint.

Consequently, from all of our above studies, laser remelted MIG welding is proved to be viable for the production of low carbon mild steel.

References

1 Cao X, Wanjara P, Munro C & Nolting A, *Mater Des*, 32 (2011) 3399.

2 Wei S & Lu S, *Mater Des*, 35 (2012) 43.

3 Sha Q, Li D, Huang G & Guan J, *Int J Miner Metall Mater*, 20 (2013) 741.

4 Ming Gao, Xiaoyan Zeng, Jun Yan & Qianwu Hu, *Appl Surf Sci*, 254 (2008) 5715.

5 Aniket Narwadkar & Santosh Bhosle, *Mater Manuf Processes*, 31 (2016) 2158.

6 Behole S D, Nemade J B, Collins Z & Liu C, *J Mater Process Technol*, 173 (2006) 92.

7 Wu C S, Hu Z K & Zhang Y M, *Proc Inst Mech Eng B, J Eng Manuf*, 223 (2009) 751.

8 Chen Y, Feng J, Li L, Chang S & Ma G, *Mater Sci Eng A*, 582 (2013) 284.

9 Kou Sindo,*Welding Metallurgy, second ed*; (Wiley-Interscience Publication: New Jersey) 2002.

10 Cheng Hongmao, Liu Fencheng, Yang Guang, Zhong Chao, Lin Xin & Huang Chunping, *Rare Metal Mat Eng*, 47 (2018) 2949.

11 Lei Zhenglong, Bi Jiang, Li Peng, Li Qian, Chen Yanbin & Zhang Dengming, *Opt Laser Technol*, 108 (2018) 409.

12 Jia Lui, Hongyin Zhu, Zhong Li, Wenfu Cui & Yan Shi, *Opt Laser Technol*, 119 (2019) 105619.

13 Xinjie Di, Shengjie Deng & Baosen Wang, *Mater Des*, 66 (2015) 169.

14 Tao Yuan, Sindo Kou & Zhen Luo, *Acta Mater*, 106 (2016) 144.

15 Rishav Sen, Choudhury S P, Ramanuj Kumar & Amlana Panda, *Mater Today Proc*, 5 (2018) 17792.

16 Gural A, Bostan B & Ozdemir A T, *Mater Des*, 28 (2007) 897.

17 Senthil kumar T, Balasubramanian V& Sanavullah M Y, *Mater Des*, 28 (2007) 2080.

18 Devendranath Ramkumar, Arun Narenthiran, Anish Konjenti, Pranav Nikam Pravin & Kanish T C, *J Mater Process Technol*, 274 (2019) 116296

19 Dongsheng Wang, Zongjun Tian, Lida Shen, Zhidong Liu & Yinhui Huang, *Ceram Int*, 40 (2014) 8791.

20 Wang Y, Li C G, Tian W & Yang Y, *Appl Surf Sci*, 255 (2009) 8603.

21 Yilbas B S, Akthar S S, Matthews A & Karatas C, *Mater Manuf Processes*, 26 (2011) 1277.

22 Iwaszko J & Nitkiewicz Z, *Mater Manuf Processes*, 17 (2002) 169.

23 Cui C Y, Cui X G, Ren X D, Liu T T, Hu J D & Wang Y M, *Mater Des*, 49 (2013) 761.

24 Shu Zhen, Zhenzhen Duan, Daqian Sun, Yexiong L I, Dandan Gao & Hongmei L I, *Opt Laser Technol*, 59 (2014) 11.

25 Mei Lifang, Yan Dongbing, Yi Jiming, Chen Genyu & Ge Xiaohong, *Mater Des*, 49 (2013) 905.

26 Sakthivel T, Vasudevan M, Laha K, Parameswaran P, Chandravathi KS, Mathew M D & Bhaduri A K, *Mater Sci Eng A*, 528 (2011) 6971.

27 Shaohua Yan, Yuan Nie, Zongtao Zhu, Hui Chen, Guoqing Gou, Jinpeng Yu & Guiguo Wan, *Appl Surf Sci*, 298 (2014) 12.

28 Lakshminarayanan A K, Balasubramanian V & Salahuddin M, *J Iron Steel Res Int*, 17 (2010) 68.

29 Caiwang Tan, Liqun Li, Yanbin Chen & Wei Guu, *Mater Des*, 49 (2013) 766.